

# ENGINE CLUTCH TORQUE ESTIMATION FOR PARALLEL-TYPE HYBRID ELECTRIC VEHICLES

J. OH<sup>1)</sup>, S. B. CHOI<sup>1)\*</sup>, Y. J. CHANG<sup>2)</sup> and J. S. EO<sup>2)</sup>

<sup>1)</sup>Mechanical Engineering Department, KAIST, Daejeon 34141, Korea

<sup>2)</sup>Eco-vehicle Control System Development Team, Hyundai Motor Company, 150 Hyundaiyeonguso-ro, Namyang-eup, Hwaseong-si, Gyeonggi 18280, Korea

(Received 30 December 2015; Revised 28 June 2016; Accepted 4 July 2016)

**ABSTRACT**—This paper mainly focuses on the accurate estimation of the torque transferred through the engine clutch installed between the engine and the drive motor in parallel-type hybrid electric vehicles. The estimation of the engine clutch torque primarily relies on the forward-direction observer which uses the nominal engine net torque information. To overcome the limitation of using the nominal engine torque information that it may not be accurate during the transient states or due to the influence of external disturbance such as the road condition and wind, the forward-direction observer is supplemented by the use of reverse-direction observer which uses the driveline model and wheel speed measurements. In addition, the drive motor torque information is used to calibrate the nominal engine torque during the idle charging state, so that the driveline characteristic unique to parallel-type hybrid electric vehicle can be utilized to increase the estimation accuracy. Finally, the estimation performance of the designed observer is tested via simulation and experiments based on a real vehicle.

**KEY WORDS** : Hybrid electric vehicle, Engine clutch, Torque observer, Estimation

## NOMENCLATURE

$\omega$	: speed
$T$	: torque
$J$	: inertia
$\alpha_{th}$	: throttle angle
$\theta$	: shaft angle
$k$	: torsional stiffness
$b$	: torsional damping coefficient
$i_t$	: transmission gear ratio
$i_f$	: final reduction gear ratio

## SUBSCRIPTS

$\hat{\cdot}$	: estimation
e	: engine
d	: damper
ec	: engine clutch
m	: drive motor
c	: transmission clutch
t	: transfer shaft
o	: output shaft
w	: wheel
v	: vehicle
1	: first clutch
2	: second clutch

## 1. INTRODUCTION

As the environmental regulations on the production of ground vehicles are growing more strict, great emphasis on the automotive technology especially related to the hybridization and electrification of powertrain (Kim *et al.*, 2015; Yoon *et al.*, 2013; Shin *et al.*, 2014) has been placed. Such increased attention on the hybrid vehicles has hence inspired the related industries to develop effective control strategies unique to the hybrid driveline to possess competitiveness in the market, and this largely concerns the engine clutch engagement control in parallel-type hybrid electric vehicle to optimize the clutch heat dissipation and jerk which directly relate to fuel efficiency and ride quality (Fredriksson and Egardt, 2000; Horn *et al.*, 2003).

The scope of this work encompasses the estimation of the engine clutch torque. Here, the engine clutch is a dry-type clutch located between the engine flywheel and the drive motor in the parallel-type hybrid electric vehicle. The engagement of this clutch enables the engine to add torque to the driveline, whereas the disengagement implies that only the drive motor is used to drive the vehicle. The ability to accurately estimate the clutch-transferred torque is crucial, since robust slip phase control of the engine clutch engagement for optimized fuel efficiency and ride quality is achievable only through feedback control strategy.

Previous attempts to realize such estimator have been made for the application on the automated manual

---

\*Corresponding author. e-mail: sbchoi@kaist.ac.kr

transmission (AMT), whose structure is similar to that of the system of interest for the fact that they both involve a single dry clutch attached to the engine flywheel. For instance, Kalman filter-based observers are designed (Pettersson, 1997; Pettersson and Nielsen, 2000, 2003; Webersinke *et al.*, 2008), but their estimation performance is limited by the linearized models. The Luenberger observer-based estimation schemes (Yi *et al.*, 1999; Shin *et al.*, 2000) overlooked the effects of the nominal engine torque and vehicle inertia uncertainties. Also, the sliding mode observer in Misawa and Hedrick (1992) and Zhao *et al.* (2013) and unknown input observers proposed in Johnson (1976) and Kim *et al.* (2012) involve chattering and phase lag issues. The actuator dynamics-based engine clutch torque estimation method is proposed (Park, 2013), and it uses the actuator current values to compute the clutch torque by tuning the model parameters such as kissing point and linear gain by learning control. However, such strategy is only able to compute the clutch torque indirectly through identifying the engagement force.

Hence, this work suggests a system of observer designed based on the driveline dynamics, which enables the real-time estimation of the engine clutch torque which has resolved the issues of nominal engine torque error and phase lag through proposing a strategy to merge two types of estimators with a variable gain. The structure of the proposed work is as follows. Section 2 first describes the model of the driveline used for the observer design. Section 3 presents the two major types of engine clutch torque estimators along with the strategy to merge them. Section 3 also includes a method for nominal engine torque scaling which compensates the long-term disturbance affecting the nominal engine torque model. Section 4 then focuses on the verification of the proposed work through simulation, and section 5 finally displays the estimation performance obtained through a real car experiment.

## 2. DRIVELINE MODEL

The driveline model used for the design of estimators and the formation of the simulation environment can be graphically represented as shown in Figure 1. As shown,

the drive motor is placed between the engine and the transmission so that the drive motor can add driving torque to the parallel-type hybrid driveline. The transmission basically takes the form of a dual clutch transmission.

Using the torque balance relationships, the driveline model shown in Figure 1 can be mathematically represented as shown next.

$$J_e \dot{\omega}_e = T_e - T_d \quad (1)$$

$$J_d \dot{\omega}_d = T_d - T_{ec} \quad (2)$$

$$J_m \dot{\omega}_m = T_{ec} + T_m - T_{c1} - T_{c2} \quad (3)$$

$$J_{e1} \dot{\omega}_{c1} = T_{c1} + T_{c2} \frac{i_{t2} i_{f2}}{i_{t1} i_{f1}} - \frac{T_o}{i_{t1} i_{f1}} \quad (4)$$

$$J_{e2} \dot{\omega}_{c2} = T_{c2} + T_{c1} \frac{i_{t1} i_{f1}}{i_{t2} i_{f2}} - \frac{T_o}{i_{t2} i_{f2}} \quad (5)$$

$$J_v \dot{\omega}_w = T_o - T_v \quad (6)$$

Here, since the dual transfer shafts in the transmission model are represented as a lumped rotating mass,  $J_{e1}$  and  $J_{e2}$  refer to the effective transmission inertia from clutch 1 and 2 perspective, respectively. In other words, either one of the torque balance equations shown in (4) and (5) can be used for the computation of the driveline states. The wheel speed refers to the processed rotational speed which can be obtained by assuming that no speed difference exists between the two ends of the differential gear. For each dynamics, the related torque is modeled as follows.

$$T_e = f(\alpha_{th}, \omega_e) \quad (7)$$

$$T_d = k_d (\theta_e - \theta_d) + b_d (\omega_e - \omega_d) \quad (8)$$

$$T_{ec} = F_{n,ec} C_{c,ec} \mu \text{sgn}(\omega_d - \omega_m) \quad (9)$$

$$T_{c1} = F_{n1} C_{c1} \mu \text{sgn}(\omega_m - \omega_{c1}) \quad (10)$$

$$T_{c2} = F_{n2} C_{c2} \mu \text{sgn}(\omega_m - \omega_{c2}) \quad (11)$$

$$T_o = k_o \left( \frac{\theta_c}{i_t} - i_t \theta_w \right) + b_o \left( \frac{\omega_c}{i_t} - i_t \omega_w \right) \quad (12)$$

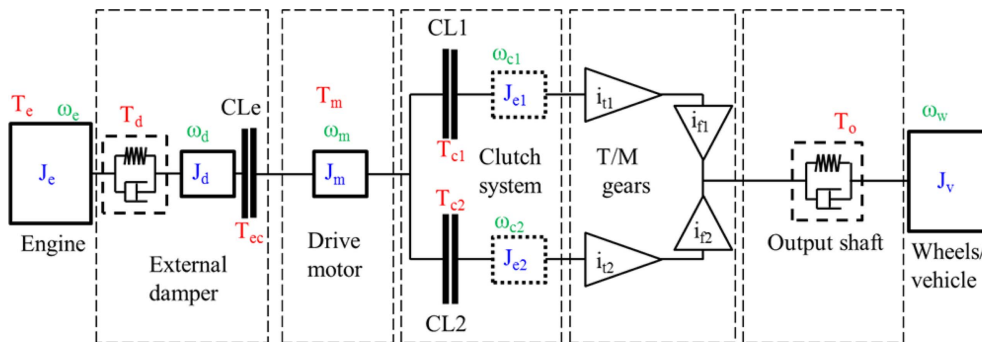


Figure 1. Representation of the driveline model used for the design of estimators.

$$T_v = r_w \left( \underbrace{m_v g \sin(\theta_{\text{road}})}_{\text{road gradient}} + \underbrace{K_{\text{rr}} m_v g \cos(\theta_{\text{road}})}_{\text{rolling resistance}} + \underbrace{\frac{1}{2} \rho v_x^2 C_d A}_{\text{aerodynamic drag}} \right) \quad (13)$$

Here,  $F_n$ ,  $C_c$ ,  $\mu$ ,  $r_w$ ,  $\theta_{\text{road}}$ ,  $K_{\text{rr}}$ ,  $m_v$ ,  $\rho$ ,  $v_x$ ,  $C_d$ , and  $A$  indicate the clutch normal force, clutch effective area, clutch friction coefficient, wheel radius, road gradient angle, tire rolling resistance, vehicle mass, air density, vehicle velocity, aerodynamic drag coefficient, and vehicle frontal area, respectively.

The engine torque (7) is determined based on the empirically obtained relationship between the engine load conditions and produced net torque. The damper torque (8) and the output torque (12) are expressed using the torsional compliance model involving spring constant and damping effect. The clutch torques (9) ~ (11) are expressed using the simple friction model where the torque is given as a function of clutch normal force and nominal friction coefficient.

The vehicle resistance torque (13) is the sum of the effects of road gradient, tire rolling resistance, and aerodynamic drag.

The transmission clutch torques carry less importance, because the engagement control of the engine clutch takes place only when launching or gear shifts are completed.

### 3. OBSERVER DESIGN

The proposed engine clutch torque observer is comprised of two parts: forward-direction torque estimation and reverse-direction torque estimation. In the forward-direction torque estimation, the input of the observer is the nominal engine torque, and the output of the observer is, of course, the engine clutch torque. Hence, the input and the output of the observer lies in the forward direction of the usual torque transmission in the driveline.

In contrast, the reverse-direction torque estimation uses the wheel speed measurement as the input and the estimated engine clutch torque as the output of the observer. Hence, the direction of estimation is the opposite of the direction of usual torque transmission in the driveline.

These two estimators are merged to operate in a supplementary manner, so that the final estimation accuracy is improved.

#### 3.1. Forward-direction Estimation

Recall Equation (2). Assuming that the difference between the engine speed and the external damper speed is negligible as well as the nominal engine torque and the damper torque, the following relationship can be reached.

$$J_d \dot{\omega}_e = T_{e,n} - T_{ec} \quad (14)$$

Based on Equation (14), the engine clutch torque can be directly computed by using the time-derivative of the engine speed measurement. However, such method

inevitably induces noise.

Hence, by considering the engine clutch torque as the unknown input (Kim *et al.*, 2012; Oh *et al.*, 2014; Oh and Choi, 2015), a simple PI type unknown input observer can be designed with the feedback being the error of the estimated engine speed.

$$\dot{\hat{\omega}}_e = \frac{1}{J_d} T_{e,n} - \frac{1}{J_d} \hat{T}_{ec,f} + l_{f1} (\omega_e - \hat{\omega}_e) \quad (15)$$

$$\dot{\hat{T}}_{ec,f} = -l_{f2} (\omega_e - \hat{\omega}_e) \quad (16)$$

This way, the estimation of the engine clutch torque,  $\hat{T}_{ec,f}$ , can be achieved.

Since  $l_{f1}$  and  $l_{f2}$  have the roles of proportional and integral feedback gains, respectively, Equation (15) takes the form of PI-type observer, which implies that the estimated engine clutch torque includes phase lag.

To reduce the effect of the phase lag, feedforward part can be added to the observer by using the predefined map-based clutch actuator model. This is done by replacing (15) and (16) by the estimator shown next.

$$\tilde{T}_{ec,f} \equiv T_{ec,f} - T_{ec,n} \quad (17)$$

$$\hat{T}_{ec,f} = T_{ec,n} + \hat{\tilde{T}}_{ec,f} \quad (18)$$

$$\dot{\hat{\omega}}_e = \frac{1}{J_d} T_{e,n} - \frac{1}{J_d} (T_{ec,n} + \hat{\tilde{T}}_{ec,f}) + l_{f1} (\omega_e - \hat{\omega}_e) \quad (19)$$

$$\dot{\hat{\tilde{T}}}_{ec,f} = -l_{f2} (\omega_e - \hat{\omega}_e) \quad (20)$$

Here,  $T_{ec,n}$  denotes the nominal value of the engine clutch torque obtained from the predefined relationship between the clutch actuator position and torque. Since this nominal value is not the function of the feedback term, it improves the transient response of the observer.

Further improvement of the forward-direction estimation performance is possible when combined with the reverse-direction estimation, which is introduced in the following section.

#### 3.2. Reverse-direction Estimation

As mentioned earlier, the reverse-direction estimator uses the wheel speed measurements to compute the engine clutch torque. A nearly-linear relationship exists between the output shaft torque and the vehicle acceleration. Hence, the output shaft torque is clearly reflected in the wheel speed measurement, from which the transient characteristics of the engine clutch torque can be found.

From Equation (3), the following expression of the engine clutch torque can be attained.

$$T_{ec} = -T_m + J_m \dot{\omega}_m + T_{c1} + T_{c2} \quad (21)$$

Since the engine clutch actuation does not take place during the transmission gear shift, consideration of both clutch 1 torque and clutch 2 torque in Equation (21) is unnecessary. Hence, two ways of estimating the engine

clutch torque are given in Equations (22) and (23) by using Equations (4) and (5), depending on which transmission clutch is engaged.

$$\hat{T}_{ec,r} = -T_m + J_m \dot{\omega}_m + J_{e1} \dot{\omega}_{c1} + \frac{\hat{T}_o}{i_{t1} i_{r1}} \quad (22)$$

$$\hat{T}_{ec,r} = -T_m + J_m \dot{\omega}_m + J_{e2} \dot{\omega}_{c2} + \frac{\hat{T}_o}{i_{t2} i_{r2}} \quad (23)$$

In other words, when clutch 1 is engaged and clutch 2 is disengaged, the torque transferred through clutch 2 is zero, from which Equation (22) can be deduced. Likewise, when only clutch 2 is engaged, then the torque transferred through clutch 1 is zero, from which Equation (23) can be deduced.

Here, the output torque can be estimated based on Equation (6), which leads to the following.

$$\hat{T}_o = J_v \dot{\omega}_w + T_v \quad (24)$$

Now the most difficult task is to accurately estimate the vehicle load torque besides obtaining the wheel acceleration from the wheel speed measurements.

Additionally, the value of  $J_v$ , the vehicle equivalent inertia, is not always a constant. Since the vehicle inertia is affected by the vehicle weight and tire radius, the nominal value may not always accurately reflect the actual inertia.

So if satisfactory level of estimation accuracy were to be achieved solely by the use of the reverse-direction estimation, constructing additional complex estimators for the load torque should be considered – for instance, by including the carefully modeled driveline efficiencies, load inertia estimation, braking torque compensation, and etc. However, such complex compensation model is unnecessary, since the strategy to simultaneously use the forward-direction and reverse-direction estimators is given in Section 3.4 for their mutually supportive operation, which is the core contribution of the suggested work.

### 3.3. Engine Torque Scaling

Before introducing the combined estimation strategy, this section addresses the engine torque scaling, in which the nominal engine torque value is calibrated using the motor torque acquired by the drive motor current measurement. Due to the nature of internal combustion engine operation, the net torque produced by the engine is often affected by various disturbances such as long-term wear, replacement of the engine oil, variation in the ambient atmospheric pressure, and etc. Accurate compensation of such uncertainties is difficult. However, thanks to the hybridized driveline structure, surely the engine torque information can be calibrated by the use of drive motor torque, since the relationship between the torque and current in the motor is rather straightforward than the torque produced by an internal combustion engine.

Recalling Equation (21), it can be easily found that the

engine clutch torque can be computed by the use of drive motor torque. However, since the right hand side of Equation (21) includes the transmission clutch torques, engine clutch torque cannot be directly computed by only using the drive motor torque when the transmission clutches are engaged.

In contrast, when the transmission is in neutral state and no torque is transferred through either clutch of the dual clutch transmission, the dynamics between the engine clutch and the drive motor becomes much simpler, as shown next.

$$T_{ec} = -T_m + J_m \dot{\omega}_m \quad (25)$$

Using this relationship that holds when the transmission is in neutral state, the engine torque constant  $C_i$  (Choi and Hedrick, 1996) is updated.

To calibrate the raw nominal engine torque, let

$$T_{e,n} = C_i T_{e,n}' \quad (26)$$

where  $T_{e,n}'$  and  $T_{e,n}$  are raw nominal engine torque and scaled nominal engine torque, respectively.

For the update of the engine torque constant, let

$$\dot{C}_i = \gamma_s (T_{ec,m} - \hat{T}_{ec,r}) \quad (27)$$

where  $T_{ec,m}$  and  $\gamma_s$  are the engine clutch torque obtained by using Equation (25) and torque constant update gain, respectively.

Since the disturbance affecting the engine torque can be considered slowly-varying, a fairly small constant can be chosen for the torque constant update gain so that the updated law is robust against any noise or unmodeled dynamics.

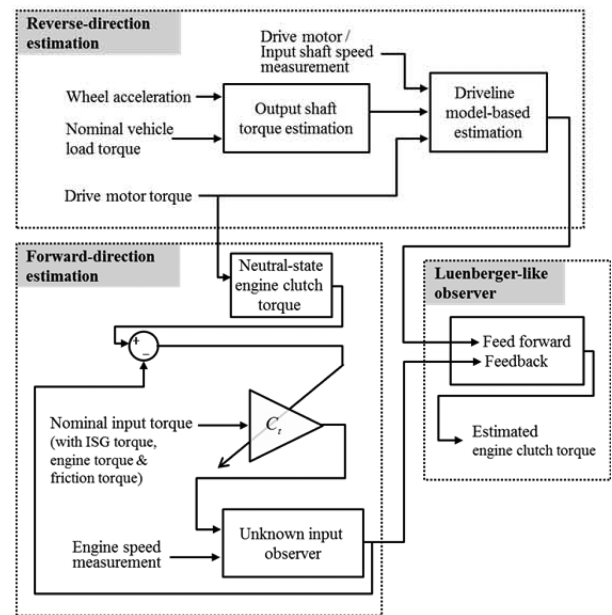


Figure 2. Block diagram representing the operation of each estimator.

Table 1. Engine clutch state depending on the battery SOC and driveline states.

Engine clutch state						
	SOC	Stop	Launch	Accel	Coasting	Brake
Charge mode	< 30	Engage	Engage	Engage	Disengage	Disengage
Normal mode	30 ~ 80	Disengage	Depends on throttle input	Depends on throttle input	Disengage	Disengage
Discharge mode	> 80	Disengage	Depends on throttle input	Depends on throttle input	Disengage	Disengage

\*Debouncing logic applied: 10 % SOC must be overcome before switching to normal mode

### 3.4. Combined Estimation

In order to acquire the final estimation of the engine clutch torque, all of the aforementioned techniques of forward-direction estimation, reverse-direction estimation, and engine torque scaling are combined in a structure with the Luenberger-like observer strategy. The basic diagram representing the operation of each part is shown in Figure 2.

The two major estimators are combined in the form of a Luenberger-like observer as shown in the following.

$$\dot{\hat{T}}_{ec} = L_{ff} \dot{\hat{T}}_{ec,r} + L_{fb} (\hat{T}_{ec,f} - \hat{T}_{ec}) \quad (28)$$

Here  $L_{ff}$ ,  $L_{fb}$ , and  $\hat{T}_{ec}$  are the feed forward gain, feedback gain, and final engine clutch torque estimation, respectively. The intermediate torque estimation results,  $\hat{T}_{ec,f}$  and  $\hat{T}_{ec,r}$ , are the outcomes of the estimators previously introduced in Section 3.1 and 3.2, respectively. The feed forward term is obtained from the result of the reverse-direction estimator so that the final estimation is less influenced by the steady-state error in  $\hat{T}_{ec,r}$ . The feedback term is obtained from the result of the forward-direction estimator so that the final estimation converges to  $\hat{T}_{ec,f}$ . This way, the final estimation has the advantage of both transient response and steady state convergence.

The feed forward gain is a value between 0 and 1, and normally, it is 1. This is for the case when the reverse-direction estimation is reliable. However, in case brake torque is applied or ABS/TCS flag is on, in order to prevent the estimation accuracy degradation, the feed forward gain is switched off and the feedback gain is increased.

## 4. SIMULATION RESULTS

### 4.1. Simulation Environment

To test the engine clutch torque estimation performance, a parallel-type hybrid electric vehicle driveline and the upper-level hybrid control algorithm is set up using a high-order driveline model based on a well-known simulation software SimDriveline. The basic structure of the primary states of hybrid control algorithm is shown in Table 1 to 3.

The plots of driveline states with the driver input and SOC for the simulation scenario are given in Figure 3. To include various conditions, the simulation scenario includes normal and discharge modes of the battery, in which all of launching, accelerating, coasting, and braking scenario are included. Also, the case of acceleration includes all of the torque flow modes: engine only, motor only, and combined. To consider practical aspects, 20 % scalar error is intentionally added to the nominal engine clutch torque value, and 10 % scalar error to the nominal value of vehicle inertia.

Table 2. Transmission clutch 1 state depending on the battery SOC and vehicle speed.

T/M Clutch 1 State		
	Stop	Others
Charge mode	Disengage	Engage
Normal mode	Engage	Engage
Discharge mode	Engage	Engage

Table 3. Modes of torque flow depending on the battery SOC and driveline states.

Torque flow					
	Stop	Launch	Accel	Coasting	Brake
Charge mode	E to G	E to G	E to G	G	G
Normal mode	M	M(+E)	M(+E)	G	G
Discharge mode	M	M(+E)	M(+E)	G	G

Legend: E – engine, M – drive motor, G – generator

\*Engine and power if torque demand > 40 %

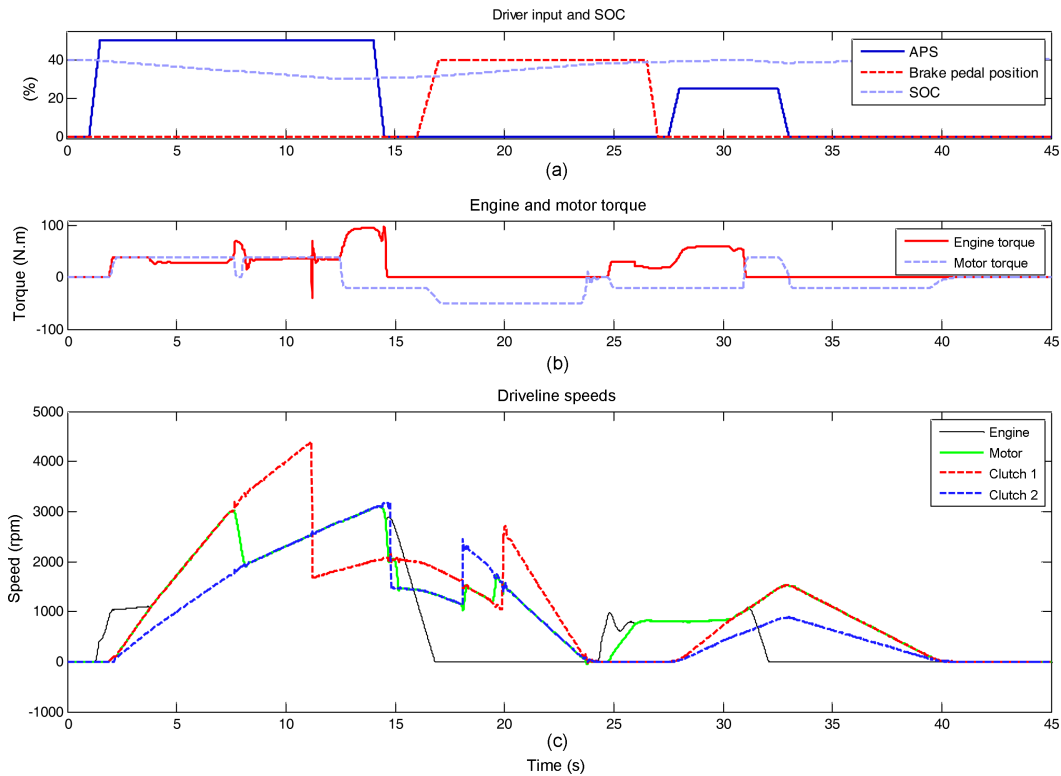


Figure 3. Plot of driver input, SOC, driving torques, and driveline speeds acquired by simulation.

Until 12 s, the vehicle accelerates by using both engine and drive motor. When the SOC drops to the level that the hybrid control unit enters the charging mode around 12 s, the vehicle only uses the engine torque to accelerate while maintaining the same level of acceleration and also distributing torque to the generator to charge the battery. At around 14 s, the vehicle stops accelerating, and starts braking at 16 s. In doing so, the motor again acts as a generator for regenerative braking. The vehicle comes to a stop at 24 s, but the engine starts for further charging. When throttle input is again demanded, the vehicle launches with the engine torque while staying in the charge mode. When the charge mode is finished at 30 s, the motor begins to produce torque once again while the engine is turned off, so that the vehicle accelerates only with the motor torque.

4.2. Estimation Performance

The nominal engine torque scaling performance is first revealed. From around 25 s to 28 s, the drive motor acts as a generator to charge the battery by using the engine torque. This indicates that the engine clutch is connected while the transmission is in neutral state. As mentioned before, this time window is when the engine torque scaling is feasible. Figure 4 shows that the uncalibrated nominal engine torque includes 20 % error, but such error is effectively eliminated in the estimation obtained by the unknown input observer based on the calibrated nominal

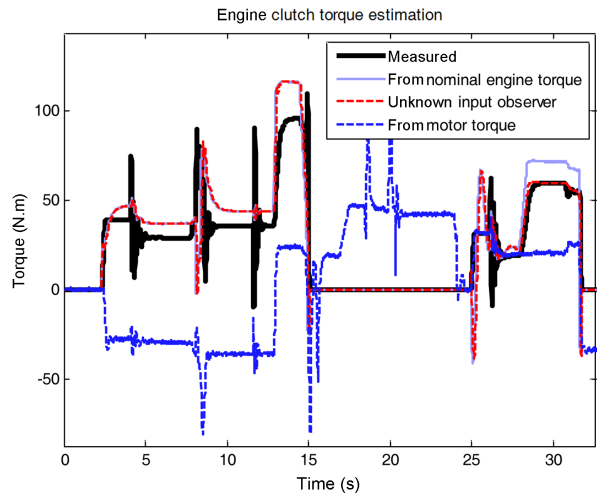


Figure 4. Comparison of engine clutch torques estimated from nominal engine torque (uncalibrated) and unknown input observer (calibrated by using neutral state motor torque).

engine torque after 28 s. This implies that engine torque scaling has effectively calibrated the raw engine torque information using the motor torque feedback. In this case of simulation, since the time window in which engine torque scaling is enabled is narrow, the torque constant update gain has been tuned so that the engine torque

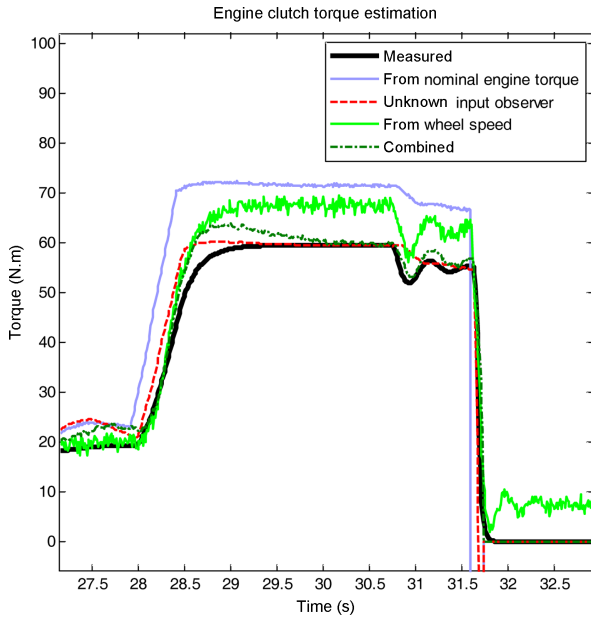


Figure 5. Comparison of estimated engine clutch torques while accelerating only with engine torque.

scaling can be completed before 28 s. However, for the realistic application in cars, the update gain may be a much lower value for stability concerns, since the range of steady state error in the raw engine torque is narrower and the error is slowly-varying.

Shown in Figure 5 are the estimated engine clutch torques. As in the case of Figure 4, scalar error can be seen in the uncalibrated nominal engine torque, while it is effectively corrected in the estimation obtained by the unknown input observer. Although this estimation is fairly accurate once the engine torque scaling has taken its effect, it cannot accurately describe the transient characteristics in the measured engine clutch torque. Such characteristic is well described by the estimation obtained by the reverse-direction estimator based on the wheel speed measurement. When such two estimation results are combined as proposed in this work, the final estimation can be obtained, which best follows after the measured value as shown in Figure 5.

The estimation results shown in Figure 6 are obtained by using the scaled nominal engine torque value for the sake of clarity in showing the effectiveness of combining the forward-direction and reverse-direction estimators.

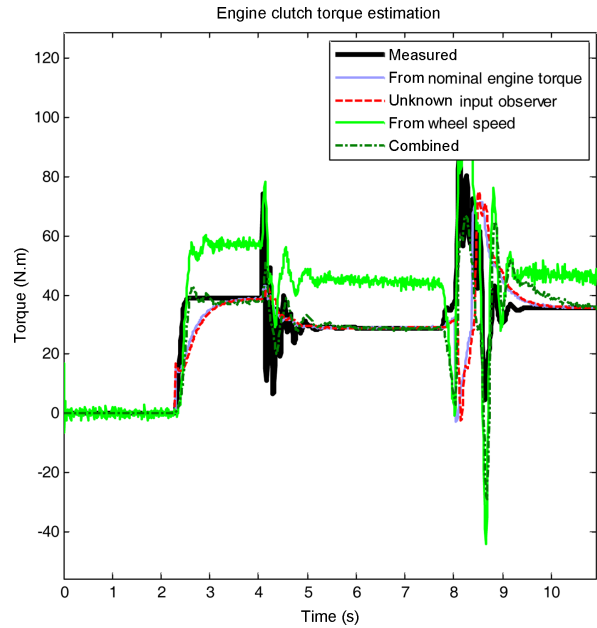


Figure 6. Comparison of estimated engine clutch torques while accelerating with both drive motor torque and engine torque.

Again, as shown in Figure 6, the result of the forward-direction estimator designed using the unknown input observer involves phase lag issue while that of the reverse-direction estimator using wheel speed information involves offset error. Such weaknesses are much resolved when the estimators are used in a combined manner, and the final estimation accurately follows the measured value as shown in Figure 6.

Overall, the estimation performance is improved relative to the case of computing the engine clutch torque from the nominal engine torque, when the forward-direction estimator is applied. This is further improved when the proposed strategy of combined forward-direction and reverse-direction estimators is used to estimate the engine clutch torque, and such result is quantitatively shown in Table 4. Here, for the sake of fair comparison, the nominal engine torque information was calibrated beforehand.

## 5. EXPERIMENT RESULTS

Due to various unmodeled dynamics of the simulation

Table 4. Quantitative comparison of estimator performance from simulation.

Estimator	1. From nominal engine torque (scaled)	2. Forward-direction estimator using unknown input observer	3. Combined (using both forward and reverse-direction estimators)
RMS error (N.m)	11.17	9.78	7.77
% improved relative to 1	-	12.4	30.4

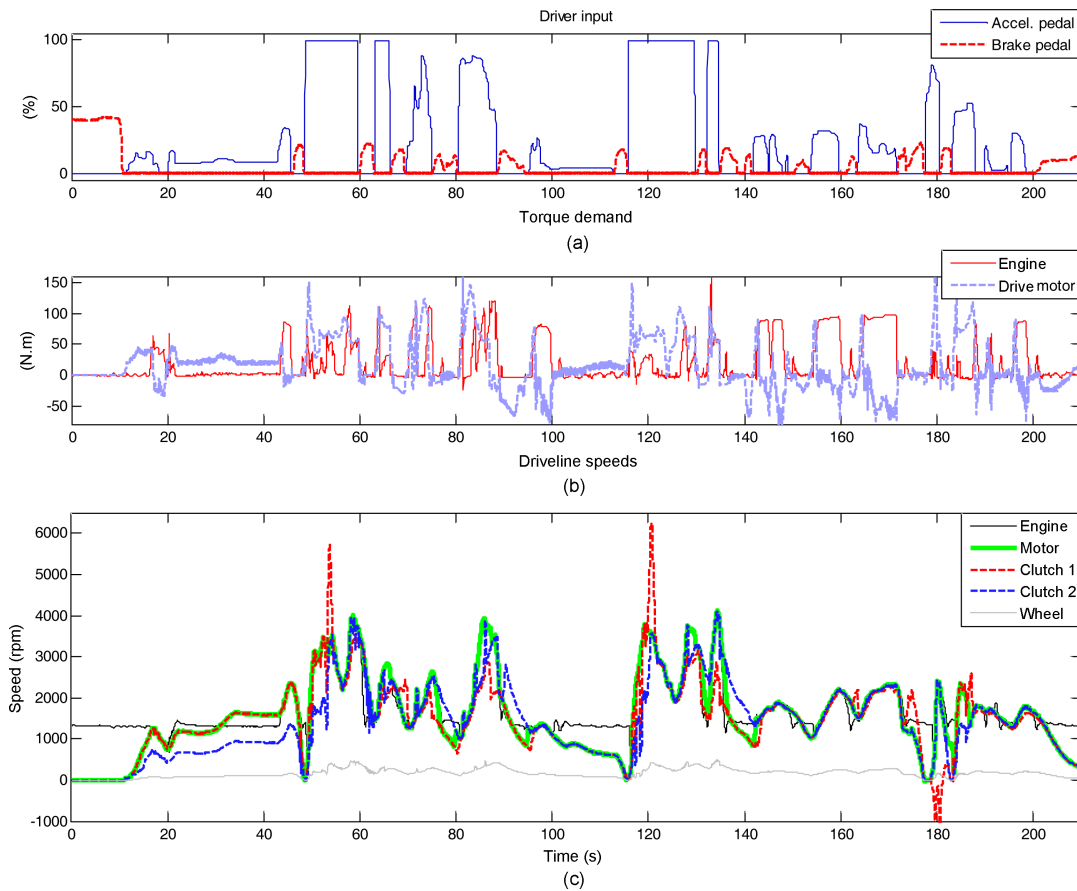


Figure 7. Plot of driver input, demand torques, and driveline speeds acquired by experiment.

environment and external sources of disturbance, the simulation alone often cannot accurately reflect the case in real vehicles. Hence, additional verification is conducted based on a real test vehicle. To compare the estimated engine clutch torque with the accurate measurement, a torque measuring device was installed at the engine flywheel.

5.1. Test Environment

Similarly to the case of simulation, a scenario which includes various conditions is selected to conduct the estimation experiment. The scenario includes vehicle launch and acceleration performed by using the engine and/or drive motor, regenerative braking, gear up/downs shifts, and wheel slipping condition during ABS/TCS operation. Details can be found in the plots shown in Figure 7.

5.2. Torque Sensor Calibration

The torque measurement sensor itself has its own rotational inertia, so its torque measurement must be compensated for such inertia effect. This is done by tuning the engine rotational inertia parameter appropriately so that the torque measurement taken by the sensor matches with the inertial torque calculated using the engine acceleration and the tuned parameter during the phase in which the engine

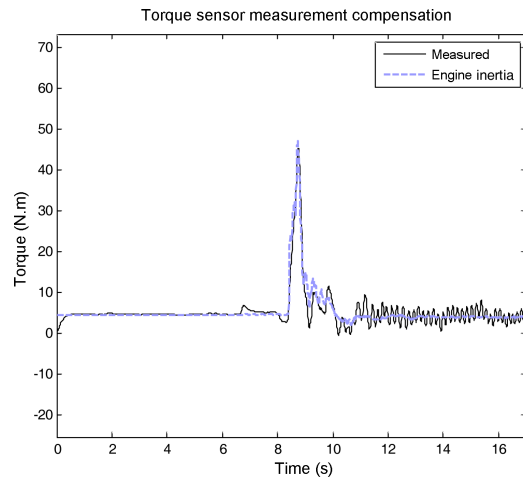


Figure 8. Plot of the raw torque measurement taken by the sensor and that for the tuned inertial torque.

clutch is completely disengaged. When this process is done, the inertial torque is subtracted from the measured torque. This way, the calibrated torque sensor measurement can accurately describe the torque transferred through the engine clutch.

The comparison between the raw torque measurement

and tuned inertial torque is displayed in Figure 8. Please notice how the plot for the raw torque measurement and that for the tuned inertial torque exactly overlap with each other. This implies that the calibrated torque measurement would turn out to be zero, which is indeed the case when the engine clutch is completely disengaged. From this point and onward, the measured engine clutch torque refers to the calibrated torque measurement.

5.3. Estimation Performance

As shown in the experiment result in Figure 9, the forward-direction estimator does not show satisfying estimation accuracy during the transient state, although its steady state offset error is fairly small. Such error is inevitable due to the incorrect nominal engine torque information obtained from the engine torque map. However, such weakness is compensated by the use of combined estimator strategy in which the reverse-direction estimator helps in improving

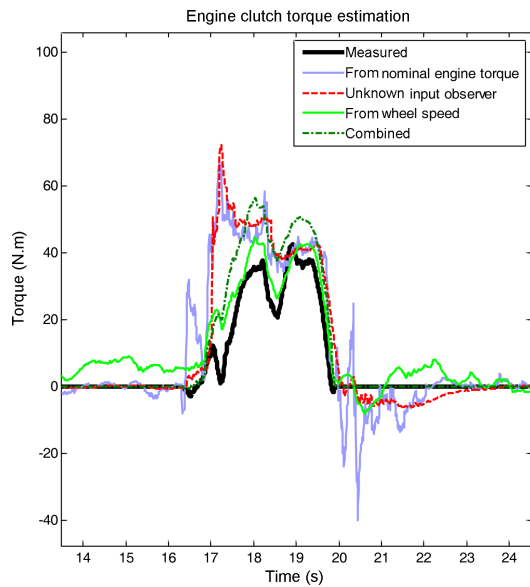


Figure 9. Comparison of estimated engine clutch torques while launching (electric mode until 16 s, and engine clutch engages between 16 s ~ 20 s).

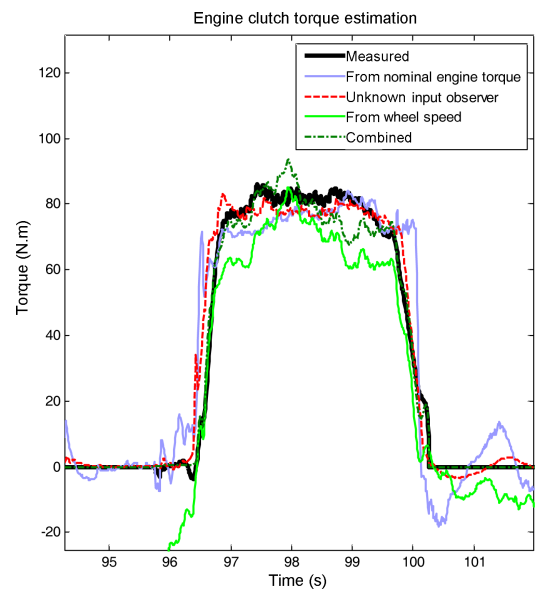


Figure 11. Comparison of estimated engine clutch torques while accelerating in presence of external disturbance affecting the vehicle load.

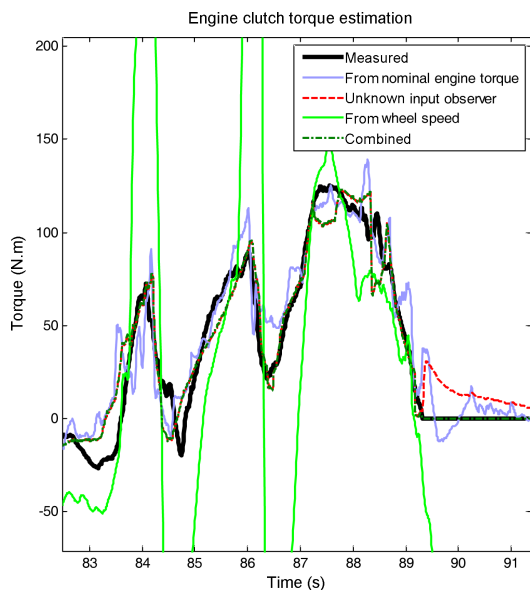


Figure 10. Comparison of estimated engine clutch torques while accelerating and causing wheel slip due to lack of tire-road friction force (TCS intervention).

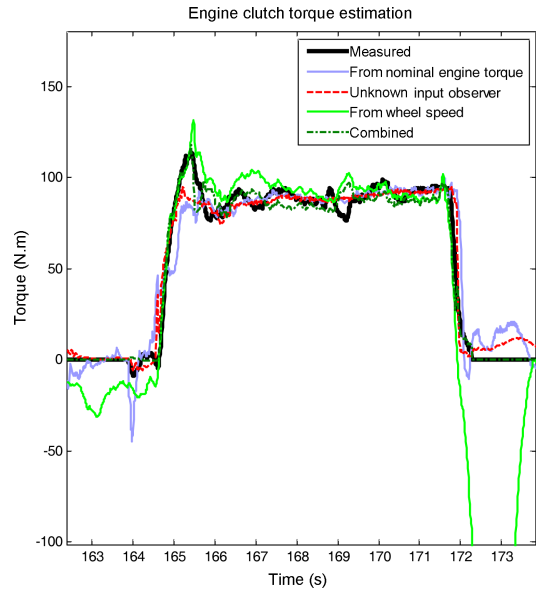


Figure 12. Comparison of estimated engine clutch torques while accelerating only with engine torque during charge mode (drive motor acting as generator).

Table 5. Quantitative comparison of estimator performance from experiment.

Estimator	1. From nominal engine torque	2. Forward-direction estimator using unknown input observer	3. Combined (using both forward and reverse-direction estimators)
RMS error (N.m)	13.66	10.42	9.07
% improved relative to 1	–	23.7	33.6

the transient state estimation performance.

In case of Figure 10, torque demand on a low-friction road surface has caused excessive wheel slip, and TCS intervention can be observed. Obviously, since the reverse-direction estimator largely relies on the wheel speed measurement, the excessive wheel slip led to degradation of the estimation performance of the reverse-direction estimator. However, the final estimation result obtained by the combine estimator maintains a fairly accurate estimation performance, thanks to the feedback provided by the unknown input observer.

Similarly, Figure 11 shows the presence of offset error in the reverse-direction estimation obtained from wheel speed information which has been caused by the external disturbance affecting the vehicle load, such as the wind or road inclination. However, such offset error barely affects the final estimation obtained by the combined estimator, again thanks to the use of unknown observer feedback.

The strength of the reverse-direction estimator is clearly shown in Figure 12, where the estimation based on the wheel speed information alone accurately describes the transient characteristic of the measured engine clutch torque at around 165 s. However, its performance turns unreliable as soon as the braking torque is applied as a disturbance to the system at 172 s, and this manifests the need for the proposed combined estimator, once again.

The quantitative performance of the entire experiment scenario in the form of RMS error is summarized in Table 5.

## 6. CONCLUSION

This study has proposed a novel strategy for estimating the torque transferred through the engine clutch placed between the engine flywheel and the drive motor in a parallel-type hybrid electric vehicle. The main contribution of this work mainly is in the strategy to combine multiple estimators. By using the forward-direction estimator using unknown input observer designed based on the engine torque dynamics, steady-state error can be eliminated, especially when combined with the technique of nominal engine torque scaling using drive motor torque during neutral gear. The phase lag issue and slow transient state estimator dynamics of such forward-direction estimator is compensated by using the reverse-direction estimator as a feed-forward part of a Luenberger-like observer, designed

based on the driveline model. With the application of the proposed estimator system which enables fast and accurate estimation of the engine clutch torque, major advancements in the driveline control for hybrid electric vehicle is anticipated, especially in the areas of fuel efficiency optimization and ride comfort improvement through the techniques of optimized slip-phase control and oscillation torque cancellation.

**ACKNOWLEDGEMENT**—This work was supported by NRF (The National Research Foundation of Korea) grant funded by the Korea government (MEST) (No. 2012-0000991) and MKE (The Ministry of Knowledge Economy), Korea, under the CITRC (Convergence Information Technology Research Center) support program (NIPA-2012-H0401-12-2003) supervised by the NIPA (National IT Industry Promotion Agency).

## REFERENCES

- Choi, S. B. and Hedrick, J. K. (1996). Robust throttle control of automotive engines: Theory and experiment. *ASME J. Dynamic Systems, Measurement, and Control* **118**, 1, 92–98.
- Fredriksson, J. and Egardt, B. (2000). Nonlinear control applied to gearshifting in automated manual transmissions. *Proc. 39th IEEE Conf. Decision and Control*, **1**, 444–449.
- Horn, J., Bamberger, J., Michau, P. and Pindl, S. (2003). Flatness-based clutch control for automated manual transmissions. *Control Engineering Practice* **11**, **12**, 1353–1359.
- Johnson, C. (1976). Theory of disturbance-accommodating controllers. *Control and Dynamic Systems*, **12**, 387–489.
- Kim, J., Oh, J. and Choi, S. B. (2012). Nonlinear estimation method of a self-energizing clutch actuator load. *Proc. Int. Conf. Innovative Engineering Systems*, 251–256.
- Kim, S. J., Yoon, Y. S., Kim, S. and Kim, K. S. (2015). Fuel economy assessment of novel multi-mode parallel hybrid electric vehicle. *Int. J. Automotive Technology* **16**, **3**, 501–512.
- Misawa, E. and Hedrick, J. (1992). Nonlinear observers – A state-of-the-art survey. *ASME J. Dynamic Systems, Measurement, and Control* **111**, **3**, 344–352.
- Oh, J. and Choi, S. B. (2015). Real-time estimation of transmitted torque on each clutch for ground vehicles with dual clutch transmission. *IEEE/ASME Trans. Mechatronics* **20**, **1**, 24–36.

- Oh, J., Kim, J. and Choi, S. B. (2014). Driveline modeling and estimation of individual clutch torque during gear shifts for dual clutch transmission. *Mechatronics* **24**, **5**, 449–463.
- Park, J. (2013). Development of engine clutch control for parallel hybrid vehicles. *World Electric Vehicle Symp. and Exhibition (EVS27)*, 1–5.
- Pettersson, M. (1997). *Driveline Modeling and Control*. Ph. D. Dissertation. Linköping University. Linköping, Sweden.
- Pettersson, M. and Nielsen, L. (2000). Gear shifting by engine control. *IEEE Trans. Control Systems Technology* **8**, **3**, 495–507.
- Pettersson, M. and Nielsen, L. (2003). Diesel engine speed control with handling of driveline resonances. *Control Engineering Practice* **11**, **3**, 319–328.
- Shin, B. K., Hahn, J. O., Yi, K. and Lee, K. I. (2000). A supervisor-based neural-adaptive shift controller for automatic transmissions considering throttle opening and driving load. *KSME Int. J.* **14**, **4**, 418–425.
- Shin, J. W., Kim, J. O., Choi, J. Y. and Oh, S. H. (2014). Design of 2-speed transmission for electric commercial vehicle. *Int. J. Automotive Technology* **15**, **1**, 145–150.
- Webersinke, L., Augenstein, L. and Kiencke, U. (2008). Adaptive linear quadratic control for high dynamical and comfortable behavior of a heavy truck. *SAE Paper No.* 2008-01-0534.
- Yi, K., Hedrick, K. and Lee, S. C. (1999). Estimation of tire-road friction using observer based identifiers. *Vehicle System Dynamics* **31**, **4**, 233–261.
- Yoon, Y. S., Kim, S. J. and Kim, K. S. (2013). Conceptual design of economic hybrid vehicle system using clutchless geared smart transmission. *Int. J. Automotive Technology* **14**, **5**, 779–784.
- Zhao, Z. G., Jiang, J. L., Yu, Z. P. and Zhang, T. (2013). Starting sliding mode variable structure that coordinates the control and real-time optimization of dry dual clutch transmissions. *Int. J. Automotive Technology* **14**, **6**, 875–888.